Aberrant activation of hepatocyte growth factor/MET signaling promotes β-catenin–mediated prostatic tumorigenesis

Received for publication, September 18, 2019, and in revised form, December 4, 2019 Published, Papers in Press, December 9, 2019, DOI 10.1074/jbc.RA119.011137

Joseph Aldahl[‡1], Jiaqi Mi[‡1], Ariana Pineda[‡], Won Kyung Kim[‡], Adam Olson[‡], Erika Hooker[‡], Yongfeng He[‡], Eun-Jeong Yu[‡], Vien Le[‡], Dong-Hoon Lee[‡], Joseph Geradts[§], and Zijie Sun[‡2]

From the Departments of [‡]Cancer Biology and [§]Population Sciences, Beckman Research Institute, City of Hope, Duarte, California 91010-3000

Edited by Alex Toker

Co-occurrence of aberrant hepatocyte growth factor (HGF)/MET proto-oncogene receptor tyrosine kinase (MET) and Wnt/β-catenin signaling pathways has been observed in advanced and metastatic prostate cancers. This co-occurrence positively correlates with prostate cancer progression and castration-resistant prostate cancer development. However, the biological consequences of these abnormalities in these disease processes remain largely unknown. Here, we investigated the aberrant activation of HGF/MET and Wnt/β-catenin cascades in prostate tumorigenesis by using a newly generated mouse model in which both murine *Met* transgene and stabilized β-catenin are conditionally co-expressed in prostatic epithelial cells. These compound mice displayed accelerated prostate tumor formation and invasion compared with their littermates that expressed only stabilized β-catenin. RNA-Seq and quantitative RT-PCR analyses revealed increased expression of genes associated with tumor cell proliferation, progression, and metastasis. Moreover, Wnt signaling pathways were robustly enriched in prostate tumor samples from the compound mice. ChIP-qPCR experiments revealed increased β-catenin recruitment within the regulatory regions of the *Myc* gene in tumor cells of the compound mice. Interestingly, the occupancy of MET on the *Myc* promoter also appeared in the compound mouse tumor samples, implicating a novel role of MET in β-catenin–mediated transcription. Results from implanting prostate graft tissues derived from the compound mice and controls into HGF-transgenic mice further uncovered that HGF induces prostatic oncogenic transformation and cell growth. These results indicate a role of HGF/MET in β-catenin–mediated prostate cancer cell growth and progression and implicate a molecular mechanism whereby nuclear MET promotes aberrant Wnt/β-catenin signaling–mediated prostate tumorigenesis.

Prostate cancer is the most common malignancy and the second leading cause of cancer mortality in men in the United States (1). Approximately 90% of patients with metastatic castrate-resistant prostate cancer (CRPC)[3] develop distal secondary bone metastasis, and nearly every patient with bone metastasis eventually succumbs to the disease, resulting in 250,000 deaths worldwide each year (2). Emerging evidence has shown the critical role of the interaction between tumor cells and their surrounding microenvironment in prostatic tumorigenesis. Hepatocyte growth factor (HGF) plays a critical role in the regulation of cell growth, cell motility, morphogenesis, and angiogenesis (3). It has been shown that HGF derived from prostate stroma significantly increases proliferation, motility, and invasion of malignant cells through its receptor, Met (4, 5). The Met receptor tyrosine kinase (RTK) is encoded by *Met*, a proto-oncogene, and has been shown to play a promotional role in the proliferation and progression of a wide variety of human malignancies, including prostate cancer (4, 6). The aberrant expression of HGF and Met often correlates with poor prognosis in cancer patients (7). HGF is abundantly expressed in the tumor microenvironment, leading to Met activation and downstream signaling that promotes several properties of tumor progression and metastasis. Up-regulation of Met expression was observed in a majority of metastatic prostate cancer lesions (6, 8–11). A nuclear form of MET, nMET, has been identified in human CRPC samples (12). Androgen deprivation can induce nMET expression and promotes cell proliferation and stemlike cell self-renewal in androgen-independent prostate cancer cells (12), implicating a novel role of Met in prostate cancer progression and CRPC development.

Whereas increased expression of Met is frequently observed in advanced and metastatic prostate cancer (13, 14), the effect of up-regulation of Met expression in the pathogenesis of prostate cancer is largely unknown. Previously, we developed a conditional *Met* transgenic mouse strain, $H11^{Met/+}$*:PB-Cre4* (15), in which the murine *Met* transgene was targeted into the *H11b* locus (16), and its expression is activated by a modified probasin

This work was supported in part by National Institutes of Health Grants R01CA070297, R01CA166894, and R01DK104941. The authors declare that they have no conflicts of interest with the contents of this article. The content is solely the responsibility of the authors and does not necessarily represent the official views of the National Institutes of Health.

This article contains Tables S1–S3 and Figs. S1 and S2.

[1] Both authors contributed equally to this work.

[2] To whom correspondence should be addressed: Rm. 2311, Beckman Bldg., Beckman Research Institute, City of Hope, Duarte, CA 91010-3000. Tel.: 626-218-0955; E-mail: zjsun@coh.org.

[3] The abbreviations used are: CRPC, castration-resistant prostate cancer; HGF, hepatocyte growth factor; hHGF, human HGF; nMET, nuclear MET; PIN, prostate intraepithelial neoplasia; HGPIN, high-grade PIN; LGPIN, low-grade PIN; AR, androgen receptor; PB, probasin; CK, cytokeratin; DEGs, differentially expressed genes; RTK, receptor tyrosine kinase; SF, scatter factor; qPCR, quantitative PCR; H&E, hematoxylin and eosin.

promoter-driven Cre expression (17). *H11*$^{Met/+}$*:PB-Cre4* mice only developed low-grade prostatic intraepithelial neoplasia (PIN) with exogenous HGF administration but failed to develop prostate carcinomas (15), suggesting that other additional factors may be required in initiating prostate tumor development.

Wnt signaling pathways play a significant role in prostate tumorigenesis (18, 19). Aberrant activation of Wnt signaling pathways was revealed as one of the most frequent abnormalities in advanced human prostate cancer (20). Abnormal expression of Wnt ligands, receptors, and effectors has been identified in prostate tumors and surrounding cells, suggesting paracrine regulatory mechanisms in prostate tumorigenesis (21, 22). Castration can elevate Wnt signaling and promote cell survival in the mouse prostate (23). An increase in nuclear β-catenin expression has been shown to promote prostate cancer cell proliferation (24). Conditional expression of stabilized β-catenin in prostate epithelium induces the development of squamous metaplasia and PIN (25, 26). An interaction between the androgen receptor (AR) and β-catenin proteins has been shown in prostate cancer cells (27–29). Interestingly, it has been shown that nMET regulates SRY (sex-determining region Y)-box9, β-catenin, and Nanog homeobox proteins predominately in CRPC cells (12).

Aberrant activation of HGF/Met and Wnt/β-catenin signaling pathways has been observed in advanced and metastatic prostate cancers and positively correlates with prostate cancer progression and CRPC development (20, 30). However, the biological roles of these abnormalities in prostate cancer progression and CRPC development are still largely unknown. In this study, we developed a compound mouse line through intercrossing our previously developed *H11*$^{Met/+}$ mouse strain with *Ctnnb1*$^{(Ex3)L/+}$*:PB-Cre4 mice* (15, 31), in which conditional expression of both murine *Met* transgene and stabilized β-catenin simultaneously co-occur in prostatic epithelial cells. The *H11*$^{L\text{-}Met/+}$*:Ctnnb1*$^{(Ex3)L/+}$*:PB-Cre4* compound mice mimic the condition of human prostate cancer cells with increased Met and β-catenin expression. Using this biologically relevant mouse model, we directly assessed the aberrant activation of HGF/Met and Wnt/β-catenin cascades in prostate tumorigenesis. The compound mice showed accelerated prostate cancer development, progression, and aggressive tumor invasion. RNA-Seq and RT-qPCR analyses showed a robust induction of β-catenin downstream target gene expression, including *Myc*, *Lef1*, *Onecut2*, *Sox2*, *Sp6*, and *Ccnd1* in samples isolated from the *H11*$^{L\text{-}Met/+}$*:Ctnnb1*$^{(Ex3)L/+}$*:PB-Cre4* compound mice compared with those from *Ctnnb1*$^{(Ex3)L/+}$*:PB-Cre4* littermate controls. Using ChIP-PCR approaches, we demonstrated increased recruitment of β-catenin within the regulatory region of the *Myc* gene in tumor cells of the compound mice. Interestingly, the occupancy of Met on the above regulator region of the *Myc* gene was also observed in the above compound mouse tumor samples, implicating the involvement of Met in β-catenin–containing transcriptional complexes. These results demonstrate a promotional role of Met in β-catenin signaling–mediated tumorigenesis and provide fresh mechanistic insight into aberrant activation HGF/Met in regulating Wnt/β-catenin activation.

Results

Development of a mouse model with conditional expression of Met and stabilized β-catenin in the mouse prostate epithelium

Both aberrant activation of HGF/MET axis and alterations in Wnt/β-catenin signaling have been observed in advanced and metastatic prostate cancers (4, 8). Recent studies further suggest that these two alterations co-exist in human prostate cancer samples (32). Aberrant activation of HGF/Met-mediated signaling pathways was detected in 158 of 2687 patients (~6%) analyzed in seven different studies (33, 34) (Fig. 1*A* and Table S1). Among those patients, ~36 patients (~23%) also bore aberrant alteration of Wnt/β-catenin signaling pathways (Fig. 1*B*). Specifically, a statistically significant correlation was revealed in the patient cohorts bearing aberrant activation of Wnt/β-catenin with abnormal HGF/MET activation (Fig. S1). Given the significance and prevalence of the HGF/Met and Wnt/β-catenin abnormalities in human prostate cancers, we generated a new mouse model, *H11*$^{L\text{-}Met/+}$*:Ctnnb1*$^{(Ex3)L/+}$*:PB-Cre4*, and directly assessed the effect of increased expression of Met and stabilized β-catenin in the mouse prostate. As detailed in Fig. 1*C*, we intercrossed *Ctnnb1*$^{(Ex3)L/+}$*:PB-Cre*4 mice (31, 35, 36) with our recently developed Met transgenic mice, *H11*$^{Met/+}$ (15) to generate the *H11*$^{L\text{-}Met/+}$*:Ctnnb1*$^{(Ex3)L/+}$*:PB-Cre4* compound mice. In this mouse model, both conditional expression of murine *Met* transgene and stabilized β-catenin co-occur simultaneously in mouse prostate epithelia (Fig. 1*C*). *H11*$^{L\text{-}Met/+}$*:Ctnnb1*$^{(Ex3)L/+}$*:PB-Cre4* and *Ctnnb1*$^{(Ex3)L/+}$*:PB-Cre*4 mice were born at the expected Mendelian ratios and appeared normal with no obvious differences from their WT littermates at birth. Using genomic PCR approaches, we assessed the presence of *PB-Cre4* as well as both the *Met* transgene and *Ctnnb1* exon 3–floxed alleles in *H11*$^{L\text{-}Met/+}$*:Ctnnb1*$^{(Ex3)L/+}$*:PB-Cre4* and *Ctnnb1*$^{(Ex3)L/+}$*:PB-Cre*4 samples. A 450-bp (Fig. 1*D*, *blue arrow*) PCR fragment, corresponding to the exon 3–targeting allele of the *Ctnnb* gene, was detected in tissues of both *H11*$^{L\text{-}Met/+}$*:Ctnnb1*$^{(Ex3)L/+}$*:PB-Cre4* and *Ctnnb1*$^{(Ex3)L/+}$*:PB-Cre*4 mice. A 340-bp fragment, corresponding to the *Met* transgene allele, was only detected in tissues of *H11*$^{L\text{-}Met/+}$*:Ctnnb1*$^{(Ex3)L/+}$*:PB-Cre4* compound mice (Fig. 1*D*, *purple arrow*). Immunoblotting analyses further demonstrated the expression of transgenic Met protein with the FLAG antibody in prostate tissues of *H11*$^{L\text{-}Met/+}$*:Ctnnb1*$^{(Ex3)L/+}$*:PB-Cre4* (Fig. 1*E*, *top*). Both endogenous and stabilized β-catenin protein were detected in prostate tissues of *H11*$^{L\text{-}Met/+}$*:Ctnnb1*$^{(Ex3)L/+}$*PB-Cre4* and *Ctnnb1*$^{(Ex3)L/+}$*:PB-Cre*4 mice (Fig. 1*E*, *middle*). The expression of both transgenic Met and stabilized β-catenin was further assessed using immunohistochemistry analyses in adjacent prostate tissue sections from age- and sex-matched *H11*$^{L\text{-}Met/+}$*:Ctnnb1*$^{(Ex3)L/+}$*:PB-Cre4* and *Ctnnb1*$^{(Ex3)L/+}$*:PB-Cre*4 mice. Cytoplasmic and nuclear β-catenin expression was detected within PIN areas in samples isolated from either *H11*$^{L\text{-}Met/+}$*:Ctnnb1*$^{(Ex3)L/+}$*:PB-Cre4* or *Ctnnb1*$^{(Ex3)L/+}$*:PB-Cre*4 (Fig. 1, *panels G* and *G′* and *panels J* and *J′*). Positive staining for Met protein was only revealed in *H11*$^{L\text{-}Met/+}$*:Ctnnb1*$^{(Ex3)L/+}$*:PB-Cre4* compound mice (Fig. 1, *K* and *K′*). The above results demonstrated the co-expression of

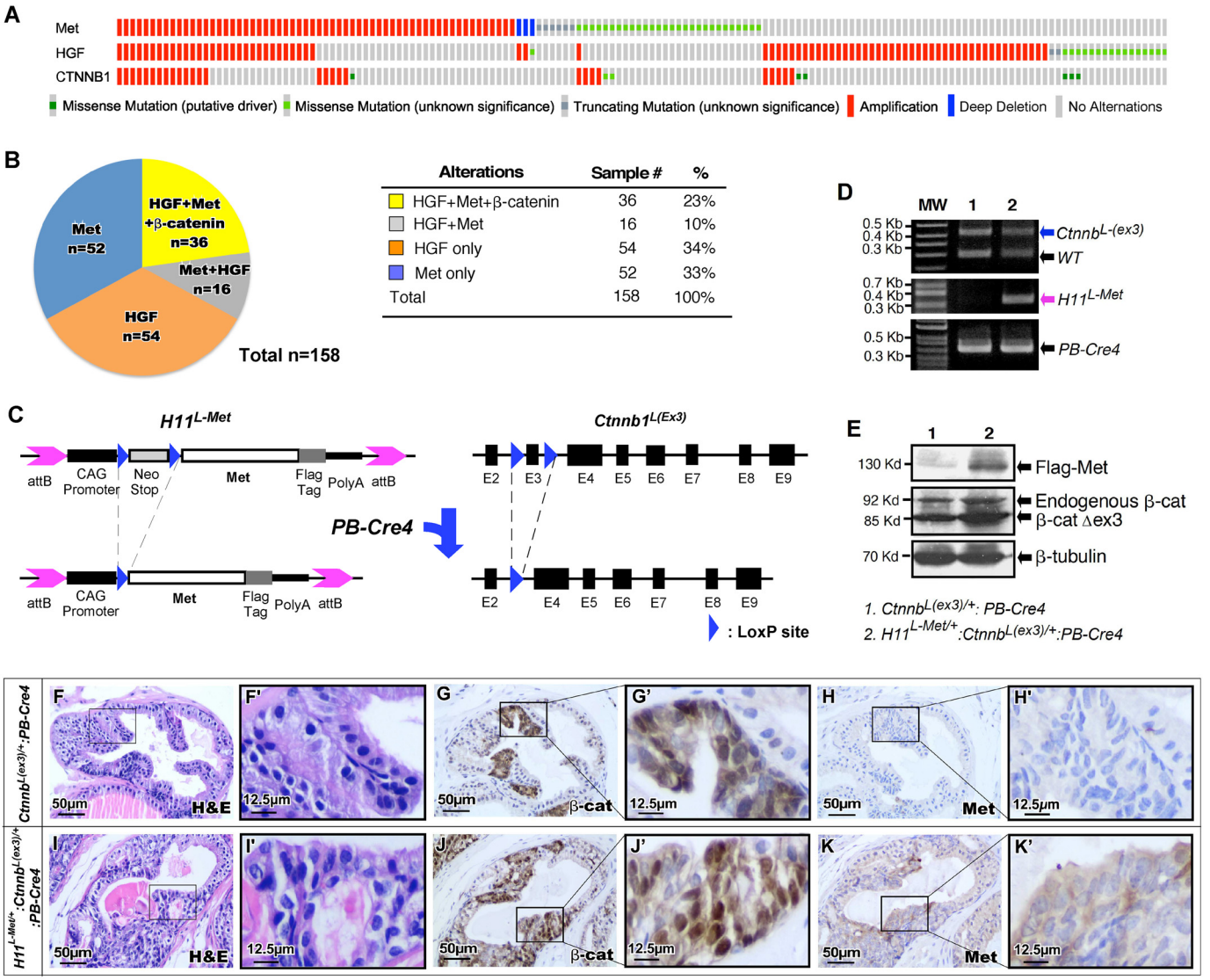

Figure 1. Generation of mice with conditional expression of Met and stabilized β-catenin in the mouse prostate. *A*, Oncoprint (http://www.cbioportal.org) (please note that the JBC is not responsible for the long-term archiving and maintenance of this site or any other third party hosted site) generated from human prostate cancer samples showing significant co-occurrence of aberrations in HGF/MET signaling pathways and aberrant alterations and mutations in *Ctnnb1*. *B*, numbers and percentages of prostate cancer samples in the patient cohort showing alterations of HGF and/or Met and β-catenin mutations. *C*, schematic of the conditional mouse Met transgene and *Ctnnb1* exon 3–targeting constructs. *Blue triangles*, LoxP sequences. *D*, genomic PCR analysis of expression of Met transgene and *Ctnnb1* exon 3–targeting allele. *E*, immunoblotting of whole prostate extracts from 6-month-old $H11^{L\text{-}Met/+}$:$Ctnnb1^{(Ex3)L/+}$:*PB-Cre4* or $Ctnnb1^{(Ex3)L/+}$:*PB-Cre4* mice with the indicated antibody. *F–J*, histological and immunohistochemical analysis of 8-week-old $H11^{L\text{-}Met/+}$:$Ctnnb1^{(Ex3)L/+}$:*PB-Cre4* or $Ctnnb1^{(Ex3)L/+}$:*PB-Cre4* mice. *F* and *I*, low and high magnification of H&E staining. Shown is immunohistochemical analysis of β-catenin (*G* and *J*) and Met (*H* and *K*) expression on sequential sections. *Scale bar*, 50 μm (12.5 μm for high-magnification images).

transgenic Met and stabilized β-catenin in the $H11^{L\text{-}Met/+}$:$Ctnnb1^{(Ex3)L/+}$:*PB-Cre4* compound mouse prostatic tissues.

Synergistic activity of MET and β-catenin accelerates mouse PIN development in the prostate

To evaluate the collaborative role of Met and stabilized β-catenin expression in the mouse prostate, we examined both $H11^{L\text{-}Met/+}$:$Ctnnb1^{(Ex3)L/+}$:*PB-Cre4* and $Ctnnb1^{(Ex3)L/+}$:*PB-Cre4* mice, adhering to recommendations of the Mouse Models of Human Cancers Consortium Prostate Pathology Committee (37). Although both $H11^{L\text{-}Met/+}$:$Ctnnb1^{(Ex3)L/+}$:*PB-Cre4* and $Ctnnb1^{(Ex3)L/+}$:*PB-Cre4* mice developed PIN lesions starting at ages of 4–6 weeks, $H11^{L\text{-}Met/+}$:$Ctnnb1^{(Ex3)L/+}$:*PB-Cre4* compound mice developed much more severe PIN lesions and revealed faster disease progression (Fig. 2, *D–F′*). Lesions in the anterior (*AP*), dorsal (*DP*), and lateral (*LP*) prostate lobes appear more severe than in the ventral prostate (*VP*) (Fig. 2, *panels D* and *D′* and *panels E* and *E′ versus panels F* and *F′*). Typical cribriform and papilliferous structures completely filled the lumen of prostatic glands of $H11^{L\text{-}Met/+}$:$Ctnnb1^{(Ex3)L/+}$:*PB-Cre4* compound mice (Fig. 2, *panels D* and *D′* and *panels E* and *E′*). In contrast, relatively mild pathological changes were observed in prostatic tissues of age-matched $Ctnnb1^{(Ex3)L/+}$:*PB-Cre4* mice (Fig. 2, *panels A* and *A′*, *panels B* and *B′*, and *panels C* and *C′*). Positive staining for stabilized β-catenin was observed in atypical cells within PIN lesions in samples of both $H11^{L\text{-}Met/+}$:$Ctnnb1^{(Ex3)L/+}$:*PB-Cre4* and $Ctnnb1^{(Ex3)L/+}$:*PB-Cre4* mice (Fig. 2, *G″* and *H″*). In addition, positive staining for Met also

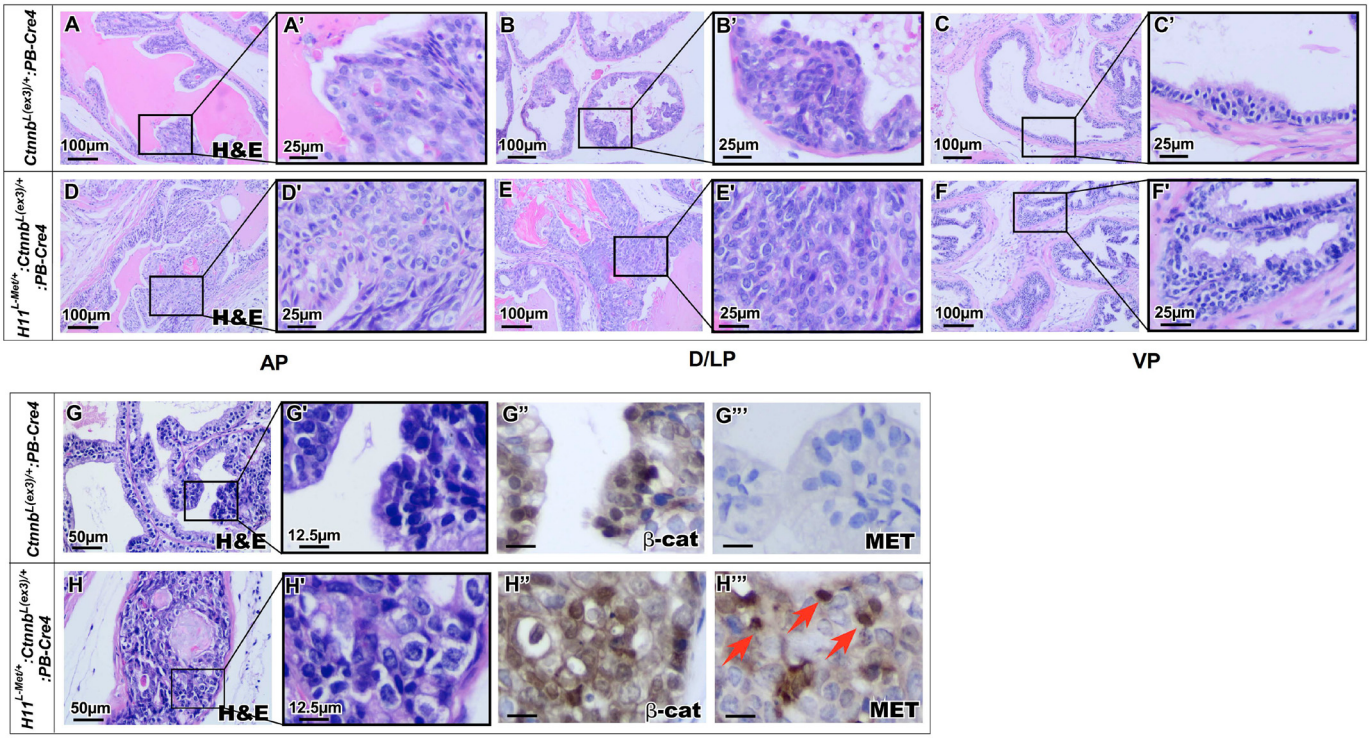

I **Pathological Abnormalities in the Prostate of *Ctnnb1$^{L(ex3)/+}$:PB-Cre4* and *H11$^{L-Met/+}$:Ctnnb1$^{L(ex3)/+}$:PB-Cre4* Mice**

Genotype	< 6 months	6 - 9 months	> 9 months
Ctnnb1$^{L(ex3)/+}$:PB-Cre4	4 of 4 LGPIN*	5 of 5 HGPIN	9 of 12 intracystic adenocarcinoma
	3 of 4 HGPIN**	3 of 5 intracystic adenocarcinoma	1 of 12 invasive adenocarcinoma
H11$^{L-Met/+}$:Ctnnb1$^{L(ex3)/+}$:PB-Cre4	5 of 5 HGPIN	4 of 4 intracystic adenocarcinoma	13 of 13 intracystic adenocarcinoma
		1 of 4 invasive adenocarcinoma	5 of 13 invasive adenocarcinoma

*LGPIN: Low grade prostatic intraepithelial neoplasia; **HGPIN: High grade prostatic intraepithelial neoplasia

Figure 2. Synergistic activity of Met and β-catenin accelerates PIN formation in the mouse prostate. *A–F*, histology of different lobes of 10-week-old *H11$^{L-Met/+}$:Ctnnb1$^{(Ex3)L/+}$:PB-Cre4* or *Ctnnb1$^{(Ex3)L/+}$:PB-Cre4* mouse prostates. *G* and *H*, immunohistochemical analysis of 10-week-old *H11$^{L-Met/+}$:Ctnnb1$^{(Ex3)L/+}$:PB-Cre4* or *Ctnnb1$^{(Ex3)L/+}$:PB-Cre4* mouse prostates with different antibodies as labeled. *I*, *table* of pathological abnormalities in the prostate of *H11$^{L-Met/+}$:Ctnnb1$^{(Ex3)L/+}$:PB-Cre4* or *Ctnnb1$^{(Ex3)L/+}$:PB-Cre4* mice. *AP*, anterior prostate; *D/LP*, dorsolateral prostate; *VP*, ventral prostate.

appeared within PIN lesions in prostate tissues of *H11$^{L-Met/+}$:Ctnnb1$^{(Ex3)L/+}$:PB-Cre4* mice (Fig. 2*H‴*) but not in those of *Ctnnb1$^{(Ex3)L/+}$:PB-Cre4* mice (Fig. 2*G‴*). These data provide a direct link between the expression of stabilized β-catenin and murine *Met* transgene with PIN development in the above mice. Interestingly, some atypical cells in *H11$^{L-Met/+}$:Ctnnb1$^{(Ex3)L/+}$:PB-Cre4* mice showed positive nuclear staining for Met (Fig. 2*H‴*, *arrows*). As age progresses, *H11$^{L-Met/+}$:Ctnnb1$^{(Ex3)L/+}$:PB-Cre4* compound mice showed faster disease progression compared with *Ctnnb1$^{(Ex3)L/+}$:PB-Cre4* mice and developed adenocarcinomas and invasive adenocarcinomas (Fig. 2*I*). The above data demonstrate a collaborative role of aberrant activation of Met and β-catenin in enhancing prostate cancer progression.

Development of invasive adenocarcinoma is promoted by Met and β-catenin expression in the mouse prostate

Our scrutiny of *H11$^{L-Met/+}$:Ctnnb1$^{(Ex3)L/+}$:PB-Cre4* compound mice revealed an invasive tumor phenotype with aggressive adenocarcinoma that occurred with much higher frequency than seen in prostatic lesions of *Ctnnb1$^{(Ex3)L/+}$:PB-Cre4* mice (Fig. 2*I*). We then continued our analysis of aged *H11$^{L-Met/+}$:Ctnnb1$^{(Ex3)L/+}$:PB-Cre4* and *Ctnnb1$^{(Ex3)L/+}$:PB-Cre4* mice up to 16 months of age. We observed that *H11$^{L-Met/+}$:Ctnnb1$^{(Ex3)L/+}$:PB-Cre4* mice developed prostatic invasive adenocarcinomas as early as 7 months of age. However, *Ctnnb1$^{(Ex3)L/+}$:PB-Cre4* mice developed less frequent invasive adenocarcinomas than the *H11$^{L-Met/+}$:Ctnnb1$^{(Ex3)L/+}$:PB-Cre4* compound mice in this cohort (Fig. 2*I*). Representative images from 12-month-old *H11$^{L-Met/+}$:Ctnnb1$^{(Ex3)L/+}$:PB-Cre4* compound mice display large, poorly differentiated carcinomas with areas of invasion (Fig. 3*B*), where the epithelial tumor cells have crossed the basement membrane into the surrounding stroma (Fig. 3 (*B1* and *B2*), *arrows*). In contrast, prostatic tumor tissues isolated from *Ctnnb1$^{(Ex3)L/+}$:PB-Cre4* mice showed pathological changes consistent with prostatic intracystic adenocarcinomas (37) (Fig. 3, *A* and *A2*). Immunohistochemistry analyses of the above tumor regions in both genotype mice showed positive staining for stabi-

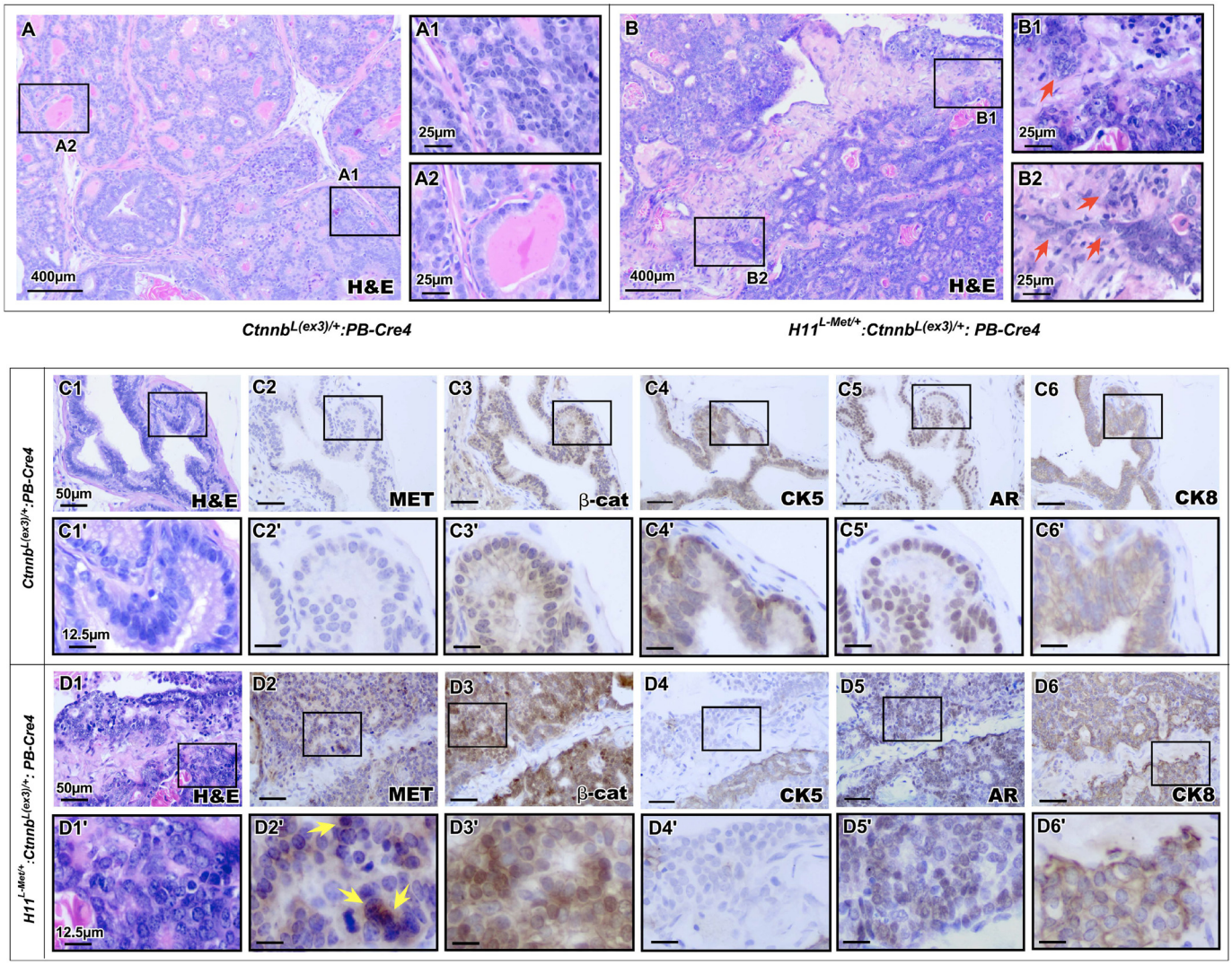

Figure 3. A collaborative role of Met and β-catenin in enhancing prostatic tumor formation and invasion. Representative histology of a 12-month-old *Ctnnb1*$^{(Ex3)L/+}$*:PB-Cre4* (*A*) or *H11*$^{L\text{-}Met/+}$*:Ctnnb1*$^{(Ex3)L/+}$*:PB-Cre4* (*B*) mouse prostate. High-magnification images show invasive prostatic adenocarcinoma (*B1* and *B2*). *C* and *D*, histological and immunohistochemical analyses of *Ctnnb1*$^{(Ex3)L/+}$*:PB-Cre4* (*C*) or *H11*$^{L\text{-}Met/+}$*:Ctnnb1*$^{(Ex3)L/+}$*:PB-Cre4* (*D*) mouse prostate using the indicated antibodies: Met (*C2* and *D2*), β-catenin (*β-cat*) (*C3* and *D3*), CK5 (*C4* and *D4*), AR (*C5* and *D5*), and CK8 (*C6* and *D6*). *Scale bars*, 400 μm (*A* and *B*), 25 μm (*panels A1* and *A2* and *panels B1* and *B2*), 50 μm (*C1–D6*), or 12.5 μm (*C1′–D6′*).

lized β-catenin (Fig. 3, *panels C3* and *C3′* and *panels D3* and *D3′*). However, positive staining for Met was only observed in prostatic tumor tissues of *H11*$^{L\text{-}Met/+}$*:Ctnnb1*$^{(Ex3)L/+}$*:PB-Cre4* compound mice (Fig. 3, *D2* and *D2′*). Interestingly, as observed previously, positive nuclear staining for Met was revealed in some tumor cells (Fig. 3*D*2′, *arrows*). Similar immunoreactivities with AR, CK8, and CK5 were observed in prostate tissues of both genotype mice (Fig. 3, *C4–C6′* and *D4–D6′*). These data further demonstrate a promotional role of transgenic Met protein in enhancing β-catenin–induced prostate tumor growth and progression.

Met enhances β-catenin–mediated tumor progression in a xenograft model

The expression of stabilized β-catenin was initiated by ARR2PB, a modified probasin promoter–driven Cre in the above compound mice (36). It has been shown that β-catenin is an AR activator and enhances AR-mediated transcription (18, 29). To reduce additional factors and specifically assess the effect of Met and stabilized β-catenin in prostate tissues, we implanted prostate tissues that were isolated from 3-week-old *H11*$^{L\text{-}Met/+}$*:Ctnnb1*$^{(Ex3)L/+}$*:PB-Cre4* and *Ctnnb1*$^{(Ex3)L/+}$*:PB-Cre4* mice under the kidney capsule of naive SCID male mice (Fig. 4*A*). The tissue grafts were harvested and analyzed after 12 weeks (Fig. 4*A*). The weight of tissue grafts derived from *H11*$^{L\text{-}Met/+}$*:Ctnnb1*$^{(Ex3)L/+}$*:PB-Cre4* was significantly higher than those from *Ctnnb1*$^{(Ex3)L/+}$*PB-Cre* littermates (Fig. 4*B*). Histological analyses of prostatic graft tissues of the compound mice showed severe pathologic changes resembling prostatic adenocarcinoma (Fig. 4*D*). Tumor cells showed cellular abnormalities, including loss of normal polarity and an increase in nuclear to cytoplasmic ratio as well as nuclear pleiomorphism (Fig. 4, *D1* and *D2*). An increase in Ki67-positive cells was also observed in prostatic graft samples of the compound mice compared with those of *Ctnnb1*$^{(Ex3)L/+}$*:PB-Cre4* mice (Fig. 4*B*). The graft tissues isolated from *Ctnnb1*$^{(Ex3)L/+}$*:PB-Cre4* mice showed less severe pathologic changes than those of the com-

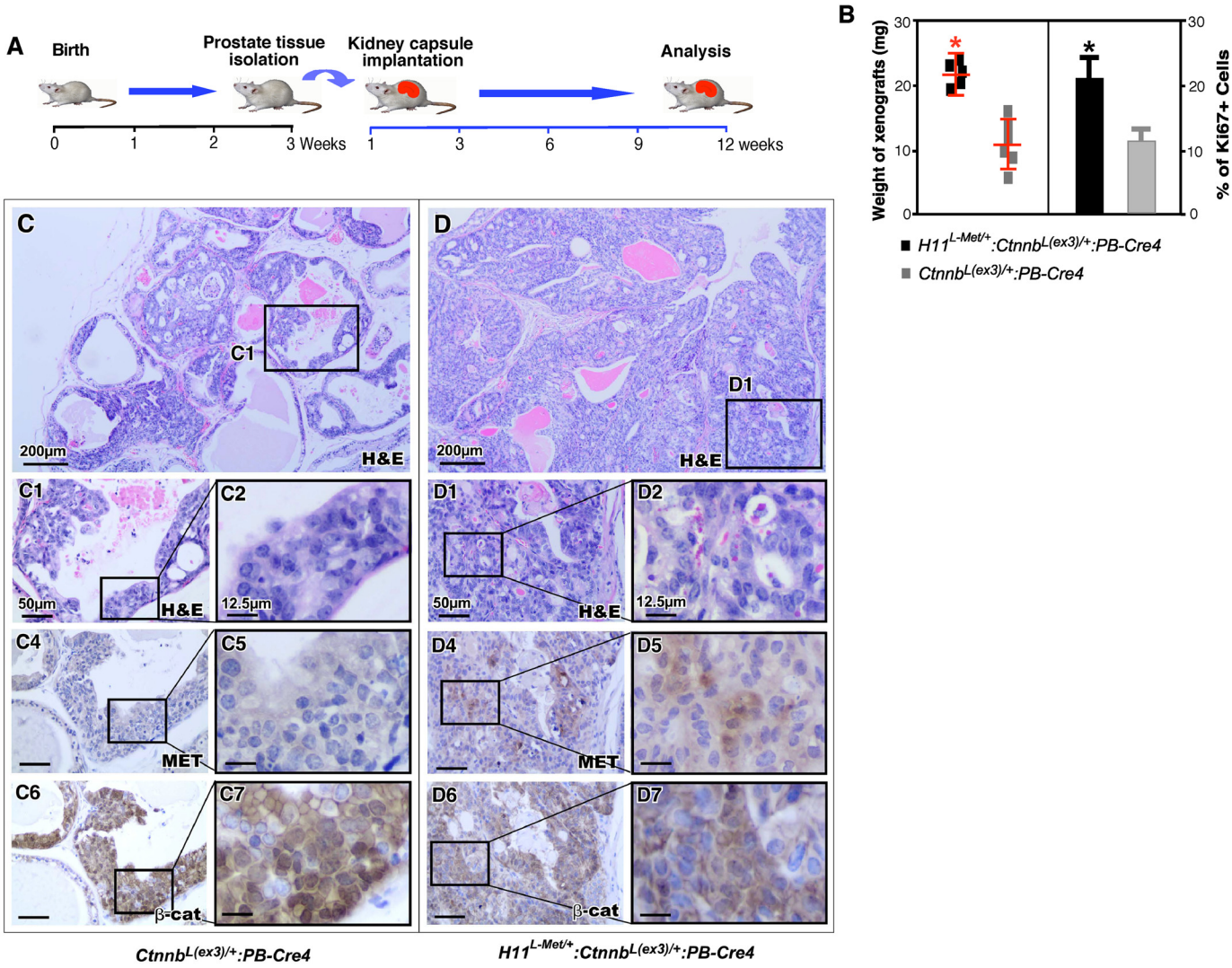

Figure 4. Met enhances β-catenin–mediated tumor progression in xenograft model for prostate cancer. *A, schematic representation* of experimental design. *B*, graphical representation of weights of xenografts derived from $H11^{L\text{-}Met/+}$:$Ctnnb1^{(Ex3)L/+}$:*PB-Cre4* or $Ctnnb1^{(Ex3)L/+}$:*PB-Cre4* mouse prostate tissues (*left*) or Ki67 expression (*right*) in prostate tissues of the indicated genotypes. Shown are representative images of H&E-stained prostate tumors from $Ctnnb1^{(Ex3)L/+}$:*PB-Cre4* (*C*) or $H11^{L\text{-}Met/+}$:$Ctnnb1^{(Ex3)L/+}$:*PB-Cre4* (*D*) mice. *C1–D2*, high-magnification images from the indicated mice. Immunohistochemical analysis of Met (*panels C4* and *C5* and *panels D4* and *D5*) and β-catenin (*panels C6* and *C7* and *panels D6* and *D7*) in prostate tissues from the indicated mice. *Scale bar*, 50 μm (12.5 μm for high-magnification images).

pound mice (Fig. 4, *C–C2*), resembling PIN lesions. Graft tissues from both genotype mice showed positive staining for β-catenin (Fig. 4, *panels C6* and *C7* and *panels D6* and *D7*). However, only graft tissues from $H11^{L\text{-}Met/+}$:$Ctnnb1^{(Ex3)L/+}$:*PB-Cre4* mice showed positive staining for Met (Fig. 4, *D4* and *D5*). These results provided an additional line of evidence demonstrating the promotional role of MET expression in enhancing stabilized β-catenin–initiated prostate tumor development and progression.

Conditional expression of Met enhances Wnt signaling to promote cellular survival, proliferation, and migration

In search of the molecular basis for the collaborative role of transgenic *Met* and stabilized β-catenin expression in prostate tumorigenesis, we performed RNA-Seq to examine the global transcriptome profiles in the tumor tissue of different genotype mice. We microscopically confirmed that the tumor tissues used to prepare RNA samples were composed of more than 80% tumor cells. Analyses of the gene expression profiles of $H11^{L\text{-}Met/+}$:$Ctnnb1^{(Ex3)L/+}$:*PB-Cre4* compared with $Ctnnb1^{(Ex3)L/+}$:*PB-Cre4* mice yielded 3240 differentially expressed genes (DEGs), of which 894 genes were up-regulated (>1 $\log_2$ -fold change) and 2346 genes were down-regulated (<−1 $\log_2$ -fold change) (Table S2). A heat map (Fig. 5*A*) depicts potential target genes that are associated with prostate differentiation and growth, tumor progression, proliferation, metastasis, and apoptosis within the context of prostate cancer (39–60) In support of our previous observations, GSEA analyses with hallmark gene sets revealed significant enrichment of the Wnt signaling pathway based on the DEGs of $H11^{L\text{-}Met/+}$:$Ctnnb1^{(Ex3)L/+}$:*PB-Cre4* *versus* $Ctnnb1^{(Ex3)L/+}$:*PB-Cre4* prostate tumor tissues (Fig. 5*B* and Table S3), suggesting a promotional role of Met in β-catenin–mediated signaling pathways. Using RT-qPCR, we further investigated the expression of β-catenin downstream target genes using RNA samples isolated

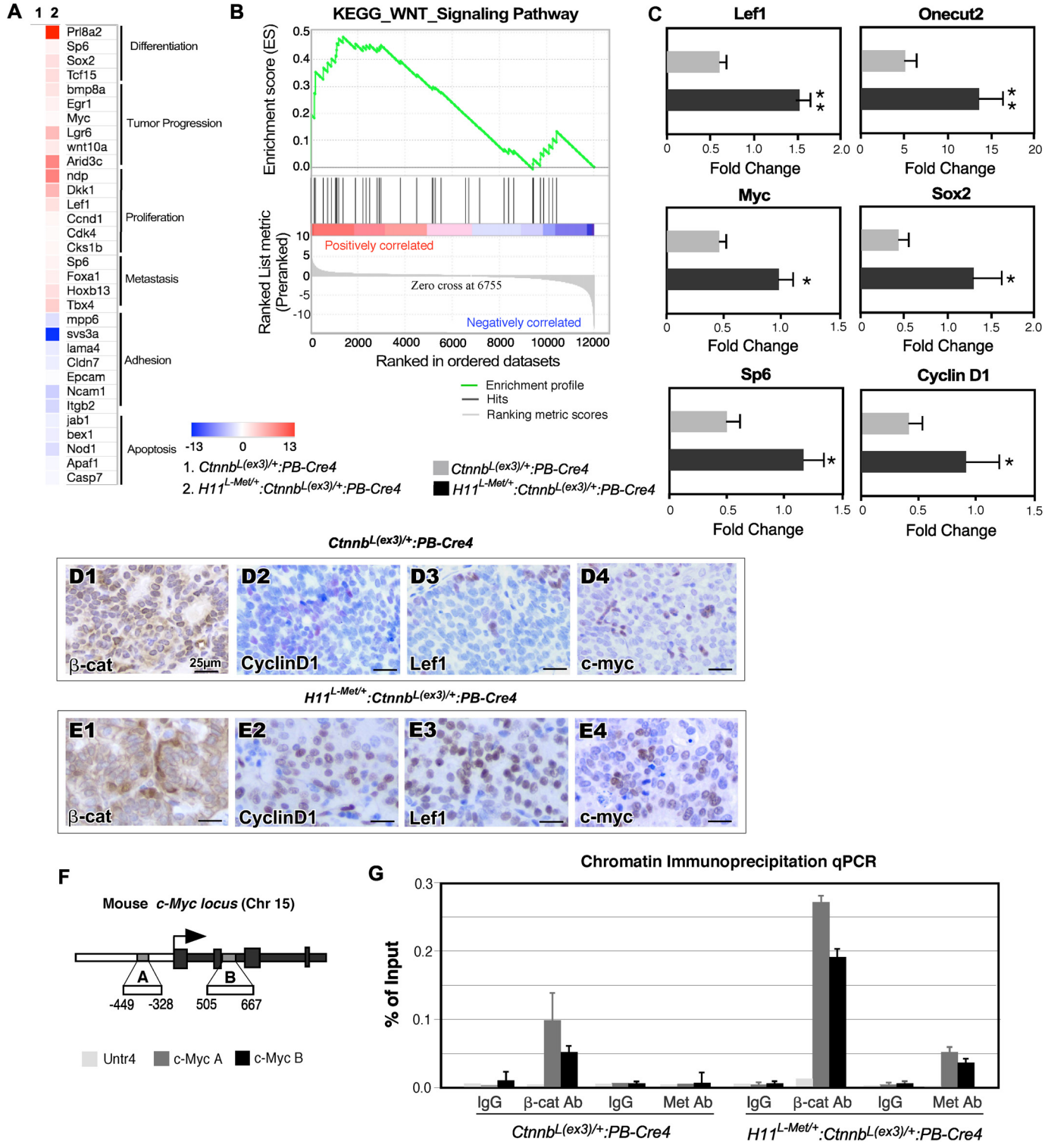

Figure 5. Conditional expression of mouse Met transgene enhances β-catenin–mediated transcription in prostatic tumor cells. *A*, heat map of representative gene sets that are altered in *Ctnnb1*$^{(Ex3)L/+}$*:PB-Cre4* and *H11*$^{L\text{-}Met/+}$*:Ctnnb1*$^{(Ex3)L/+}$*:PB-Cre4* tumors. *B*, enrichment plot for expression of genes involved in the Wnt signaling pathway. *C*, RT-qPCR validation of the gene expression in *Ctnnb1*$^{(Ex3)L/+}$*:PB-Cre4* and *H11*$^{L\text{-}Met/+}$*:Ctnnb1*$^{(Ex3)L/+}$*:PB-Cre4* tumors. The data are presented as the mean ± S.D. (*error bars*) for three independent samples: *, $p < 0.05$; **, $p < 0.01$. *D* and *E*, immunohistochemical analysis of β-catenin (*D1* and *E1*), CCND1 (*D2* and *E2*), Lef1 (*D3* and *E3*), and Myc (*D4* and *E4*) expression in prostate tumors of *Ctnnb1*$^{(Ex3)L/+}$*:PB-Cre4* and *H11*$^{L\text{-}Met/+}$*:Ctnnb1*$^{(Ex3)L/+}$*:PB-Cre4* mice, respectively. *F*, *schematic* of the two β-catenin–binding sites in the mouse *Myc* locus. *G*, chromatin immunoprecipitation qPCR results from ChIP with different antibodies and IgG using the indicated conditions. *Scale bar*, 25 μm.

from *H11*$^{L\text{-}Met/+}$*:Ctnnb1*$^{(Ex3)L/+}$*:PB-Cre4 versus Ctnnb1*$^{(Ex3)L/+}$*:PB-Cre4*. As shown in Fig. 5*C*, an increase in the expression of β-catenin downstream target genes involved in cell proliferation and tumor progression, including *Lef1*, *Myc*, *Sp6*, *Onecut2*, *Sox2*, and *Ccnd1*, was observed in RNA samples isolated from *H11*$^{L\text{-}Met/+}$*:Ctnnb1*$^{(Ex3)L/+}$*:PB-Cre4* mice compared

with those of *Ctnnb1*$^{(Ex3)L/+}$*:PB-Cre*4 littermates. Using immunohistochemistry, we further demonstrated increased expression of β-catenin, cyclin D1, Lef1, and Myc proteins in prostatic tumor samples of *H11*$^{L\text{-}Met/+}$*:Ctnnb1*$^{(Ex3)L/+}$*:PB-Cre4* mice compared with the samples of *Ctnnb1*$^{(Ex3)L/+}$*:PB-Cre*4 mice (Fig. 5, *D1–D4* and *E1–E4*). To directly determine the role of Met in β-catenin–mediated transcription, we performed ChIP-qPCR analyses using the immunoprecipitated genomic DNA samples isolated from prostatic tumor cells of *H11*$^{L\text{-}Met/+}$*:Ctnnb1*$^{(Ex3)L/+}$*:PB-Cre4* and *Ctnnb1*$^{(Ex3)L/+}$*:PB-Cre*4 mice to examine the occupancy of stabilized β-catenin and Met on the mouse *Myc* locus (Fig. 5*F*), a *bona fide* β-catenin downstream target gene (61). We observed a significant increase in recruitment of β-catenin within both binding sites in the regulatory region of the *Myc* in tumor samples isolated from *H11*$^{L\text{-}Met/+}$*:Ctnnb1*$^{(Ex3)L/+}$*:PB-Cre4* compound mice compared with the ones from *Ctnnb1*$^{(Ex3)L/+}$*:PB-Cre*4 only mice (Fig. 5*G*). However, there is no significant recruitment with IgG or on the locus of *Untr4*, used as a negative control (62). A previous report has shown a nuclear localization of Met in prostate tumor cells (12). In this study, we also observed nuclear staining of Met in prostate tumor cells of *H11*$^{L\text{-}Met/+}$*:Ctnnb1*$^{(Ex3)L/+}$*:PB-Cre4* compound mice (Figs. 2*H‴* and 3*D2′*). To further explore the potential role of Met in the nuclei of prostatic tumor cells in the above mouse models, we further examined the involvement of Met in β-catenin–mediated transcription using the above immunoprecipitated genomic DNA samples. Interestingly, we observed the occupancy of Met on both binding sites within the regulatory region of the *Myc* in tumor samples of *H11*$^{L\text{-}Met/+}$*:Ctnnb1*$^{(Ex3)L/+}$*:PB-Cre4* compound mice but not in those of *Ctnnb1*$^{(Ex3)L/+}$*:PB-Cre*4 mice (Fig. 5*G*). The recruitment of Met in β-catenin–mediated transcriptional complexes on the promoters of β-catenin–regulated downstream target genes, *Lef1* and *Ccnd1*, was also identified in the tumor samples of the above compound mice using ChIP-qPCR approaches (Fig. S2). These data suggest a potential role of Met in β-catenin–involved transcription complexes, providing new mechanistic insight into the effect of Met in promoting β-catenin–mediated tumor growth and progression.

HGF facilitates β-catenin–mediated tumor progression in a xenograft model

Met is the RTK for HGF/SF and is activated by HGF/SF (3). Conditional expression of the murine *Met* gene did not shown notable abnormalities in the prostate of *H11*$^{Met/+}$*:PB-Cre4* mice (15). In this study, we assessed the direct role of activation of Met through HGF in promoting β-catenin–mediated prostate tumor growth in *H11*$^{L\text{-}Met/+}$*:Ctnnb1*$^{(Ex3)L/+}$*:PB-Cre4* compound mice. We implanted prostate tissues isolated from 3-week-old *H11*$^{L\text{-}Met/+}$*:Ctnnb1*$^{(Ex3)L/+}$*:PB-Cre4* compound mice and their *Ctnnb1*$^{(Ex3)L/+}$*:PB-Cre*4 littermates under the kidney capsule of hHGF transgenic SCID male mice (63) (Fig. 6*A*). Examination of 6–9-week-old hHGF transgenic SCID mice showed higher levels of HGF in sera of these mice than those of age- and sex-matched BL6/C57 and regular SCID mice (Fig. 6*B*), which is consistent with the previous report (63). Gross examination showed that the grafts derived from *H11*$^{L\text{-}Met/+}$*:Ctnnb1*$^{(Ex3)L/+}$*:PB-Cre4* compound mice were larger and heavier than those derived from *Ctnnb1*$^{(Ex3)L/+}$*:PB-Cre*4 (Fig. 6, *C* and *D*). Increased Ki67-positive cells were revealed in grafts from the above compound mice than those from the controls (Fig. 6*E*). Histologically, graft tissues derived from *H11*$^{L\text{-}Met/+}$*:Ctnnb1*$^{(Ex3)L/+}$*:PB-Cre4* compound mice showed pathological lesions resembling HGPIN lesions (Fig. 6, *G–G2*). In contrast, only LGPIN lesions were revealed in graft tissues of *Ctnnb1*$^{(Ex3)L/+}$*:PB-Cre*4 mice (Fig. 6, *F–F2*). Whereas graft tissues from *H11*$^{L\text{-}Met/+}$*:Ctnnb1*$^{(Ex3)L/+}$*:PB-Cre4* and *Ctnnb1*$^{(Ex3)L/+}$*:PB-Cre*4 mice showed strong cytoplasmic and nuclear staining for β-catenin (Fig. 6, *F3* and *G3*), positive staining for Met and pMet only appeared in focal cells in grafts of the compound mice. Specifically, some cells showed clear nuclear staining of Met (Fig. 6, *G4* and *G5*, *arrows*). There was no visible staining for HGF in both graft tissues (Fig. 6, *F6* and *G6*). Positive staining for other prostate cellular markers, such as AR, CK8, and CK5, appeared in both graft tissues (Fig. 6, *F7–F9* and *G7–G9*). Taken together, these results provide direct evidence demonstrating that the activation of Met by HGF promotes β-catenin–mediated prostatic tumor growth.

Discussion

The HGF/Met signaling pathway plays a critical role in prostate tumorigenesis. Up-regulation of Met expression appeared in a majority of advanced and metastatic prostate cancer lesions (6, 8–11). In addition, aberrant activation of Wnt signaling pathways has also been shown to be one of the most frequent abnormalities in advanced human prostate cancer (20). Recent studies from human prostate cancer samples further suggest that these two alterations co-exist in human prostate cancer, particularly in the late stages of disease (32). Particularly, aberrant co-amplification and activation of Wnt/β-catenin with abnormal MET or HGF activation were also seen in the above-referenced prostate cancer samples, and an inverse correlation exists between these abnormalities and survival rates (Fig. S1). Given this biological significance and clinical relevance, we directly assessed the collaborative role of aberrant activation Met and β-catenin in prostate tumorigenesis using a newly generated mouse model, *H11*$^{L\text{-}Met/+}$*:Ctnnb1*$^{(Ex3)L/+}$*:PB-Cre4*. As described above, conditional expression of the murine *Met* gene and stabilized β-catenin co-occurred in prostatic epithelial cells of the above mice. This clinically relevant mouse model enables us to recapitulate the aberrant activation of Met and β-catenin during prostate cancer development and progression. The *H11*$^{L\text{-}Met/+}$*:Ctnnb1*$^{(Ex3)L/+}$*:PB-Cre4* compound mice showed accelerated prostate tumor development and progression compared with their *Ctnnb1*$^{(Ex3)L/+}$*:PB-Cre4* littermates, demonstrating a promotional role of the HGF/Met signaling axis in Wnt/β-catenin–mediated prostate tumorigenesis. The *H11*$^{L\text{-}Met/+}$*:Ctnnb1*$^{(Ex3)L/+}$*:PB-Cre4* compound mouse model will be a biologically relevant and useful tool for further characterizing the molecular mechanisms underlying HGF/Met signaling in prostate cancer development, progression, and metastasis.

Emerging evidence has shown the significance of the HGF/Met signaling pathway in prostate cancer progression and CRPC development (64). HGF plays a critical role in the regulation of cell growth, cell motility, morphogenesis, and angiogenesis (3). The HGF-Met signaling axis is known to be impor-

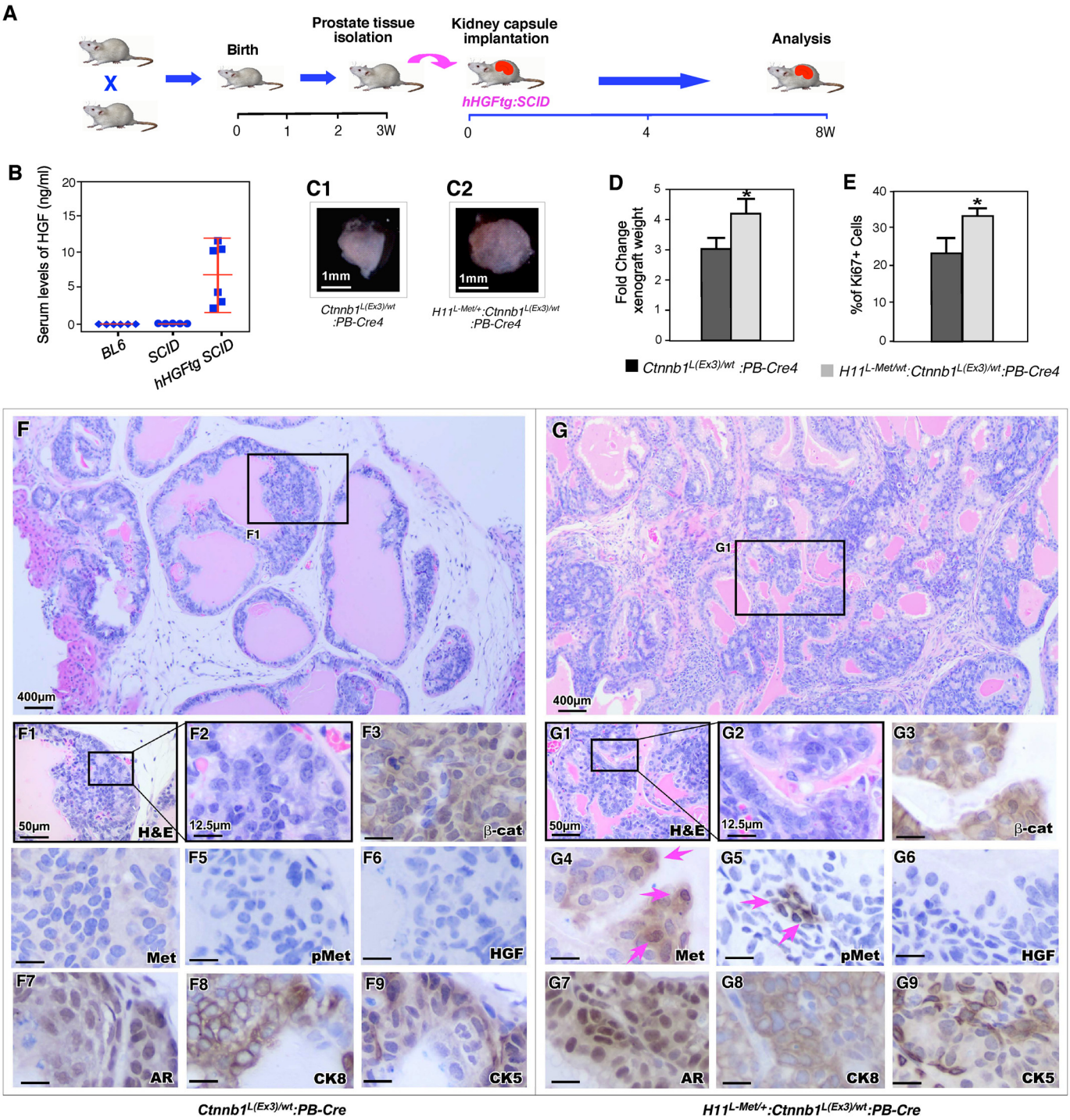

Figure 6. Expression of HGF promotes prostatic tumor formation in *H11*$^{L\text{-}}$Met$^{/+}$*:Ctnnb1*$^{(Ex3)L/+}$*:PB-Cre4* mice. *A*, *schematic representation* of experimental design. *B*, ELISA results for serum levels of HGF in mice of the indicated genotypes. *C*, representative gross images for xenografts derived from prostate tissues of the indicated genotypes. *D*, graphical representation of the average weight of xenografts from the indicated genotypes. *E*, graphical representation of Ki67 expression in xenografts derived from *Ctnnb1*$^{(Ex3)L/+}$*:PB-Cre4* and *H11*$^{L\text{-}Met/+}$*:Ctnnb1*$^{(Ex3)L/+}$*:PB-Cre4* mice. *F* and *G*, representative images of H&E-stained prostate tumors from *Ctnnb1*$^{(Ex3)L/+}$*:PB-Cre4* (F-F2) or *H11*$^{L\text{-}Met/+}$*:Ctnnb1*$^{(Ex3)L/+}$*:PB-Cre4* (G-G2) mice. Shown is immunohistochemical analysis of β-catenin (*F3* and *G3*), MET (*F4* and *G4*), phosphorylated Met (*F5* and *G5*), HGF (*F6* and *G6*), AR (*F7* and *G7*), CK8 (*F8* and *G8*), or CK5 (*F9* and *G9*) expression in prostate tumors of *Ctnnb1*$^{(Ex3)L/+}$*:PB-Cre4* and *H11*$^{L\text{-}Met/+}$*:Ctnnb1*$^{(Ex3)L/+}$*:PB-Cre4* mice, respectively. *Scale bar*, 1 mm (*C*), 400 μm (*F* and *G*), 50 μm (*F1* and *G1*), and 12.5 μm (*F2–F9* and *G2–G9*). The data are presented as the mean S.D. + (*error bars*) for three independent samples. *, $p < 0.05$.

tant to bone remodeling. An increase in expression of both the Met receptor and the HGF ligand has been observed at sites of prostate cancer bone metastasis, suggesting that this pathway may be active during bone metastasis (8). Up-regulation of Met expression has been observed in most metastatic prostate cancer lesions (6, 8–11). A significant challenge within the field of prostate cancer has been the lack of clinically relevant models for examining the biological role of Met in prostate tumor progression and metastasis. Therefore, we recently developed *H11*$^{Met/+}$*:PB-Cre4* mice, where expression of the mouse *Met*

gene is specifically activated in prostatic epithelial cells through *Cre-LoxP*–mediated recombination (15). Although activation of murine *Met* gene expression with the addition of HGF administration induced prostatic intraepithelial neoplasia development, no prostate tumor formation was revealed in $H11^{Met/+}$*:PB-Cre4* mice. These data suggest that other oncogenic hits may be required in HGF/Met signaling axis–induced prostate tumor formation and progression. Therefore, in this study, we used stabilized β-catenin mice (31), a well-established Wnt signaling tumor model, to directly assess the promotional role of Met in prostate tumor formation and progression. We observed the development of more aggressive and invasive prostate tumors in $H11^{L\text{-}Met/+}$*:*$Ctnnb1^{(Ex3)L/+}$*:PB-Cre4* compound mice compared with their $Ctnnb1^{(Ex3)L/+}$*:PB-Cre4* littermates. However, we did not observe tumor metastasis in the above compound mice. Despite the evidence indicating that HGF/Met activation is closely associated with bone metastases in human prostate cancer, the failure of metastatic prostate tumor development in the above mouse models indicates that many biological differences may exist between human and murine prostate tissues. The data collected in this study have led us to pursue several more in-depth characterizations of the HGF/Met signaling axis.

The Met is an RTK for HGF (3, 4, 6). It has been shown that Met activation through binding HGF regulates prostate cell proliferation, motility, and invasion (4, 5). Low and inconsistent levels of HGF have been reported in mice (65). To address this caveat, we implanted prostatic tissues isolated from either 3-week-old $H11^{L\text{-}Met/+}$*:*$Ctnnb1^{(Ex3)L/+}$*:PB-Cre4* or $Ctnnb1^{(Ex3)L/+}$*:PB-Cre4* mice under the kidney capsules of HGF transgenic SCID male mice (63). We analyzed graft tissues after 8 weeks of implantation, rather than the 12-week period that we routinely use. We observed robust atypical cell growth and pathologic changes resembling HGPIN lesions in grafts derived from $H11^{L\text{-}Met/+}$*:*$Ctnnb1^{(Ex3)L/+}$*:PB-Cre4* mice. In contrast, only a few local LGPIN lesions were revealed in graft tissues of $Ctnnb1^{(Ex3)L/+}$*:PB-Cre4* mice. The above pathological differences clearly reflect a promotional role of transgenic HGF expression in activating Met in inducing oncogenic transformation in the mouse prostate and promoting tumor cell growth. Establishing a new mouse strain with both transgenic HGF and Met expression may more closely mimic the pathologic conditions of human prostate cancer, and this should be developed and further investigated. Particularly, using this double transgenic mouse strain in the presence of other oncogenic hits may produce more aggressive and metastatic prostate tumor phenotypes in future mouse models.

To further understand the molecular mechanism underlying Met-mediated tumor progression and metastasis, we examined the transcriptional profile in prostate tumor tissues isolated from both $H11^{L\text{-}Met/+}$*:*$Ctnnb1^{(Ex3)L/+}$*:PB-Cre4* or $Ctnnb1^{(Ex3)L/+}$*:PB-Cre4* mice using RNA-Seq approaches. Increased expression of genes related to tumor development and progression was observed in the samples from $H11^{L\text{-}Met/+}$*:*$Ctnnb1^{(Ex3)L/+}$*:PB-Cre4* mice. An enrichment in Wnt signaling was also identified in DEGs between $H11^{L\text{-}Met/+}$*:*$Ctnnb1^{(Ex3)L/+}$*:PB-Cre4* and $Ctnnb1^{(Ex3)L/+}$*:PB-Cre4* mice, suggesting a promotional role of transgenic Met expression in enhancing β-catenin mediated transcription. An increase in β-catenin downstream target genes was further shown in tumor samples from the compound mice. Interestingly, a significant increase of Onecut2, a newly defined master regulator in prostate tumor progression (66), was revealed in tumor samples of the compound mice. A previous study has shown a nuclear form of Met in castrated Pten/Trp53 null prostate tumor cells, which can activate Sox9, β-catenin, and Nanog transcription factors (12). Using ChIP-qPCR approaches, we observed the recruitment of Met in β-catenin–involved transcription complexes on the promoters and other regulatory regions of β-catenin–regulated downstream target genes, including Myc, cyclin D1, and Lef1, in prostatic tumor cells of the $H11^{L\text{-}Met/+}$*:*$Ctnnb1^{(Ex3)L/+}$*:PB-Cre4* compound mice. Our data support the previous observation of nuclear Met and provide additional scientific evidence demonstrating a novel role of Met in facilitating β-catenin–mediated transcription in prostate cancer cells. Identification of the nuclear role of transgenic Met protein beyond its canonical role on the membrane in tumor cells of $H11^{L\text{-}Met/+}$*:*$Ctnnb1^{(Ex3)L/+}$*:PB-Cre4* is novel and interesting. Further characterization of nuclear Met using $H11^{L\text{-}Met/+}$*:*$Ctnnb1^{(Ex3)L/+}$*:PB-Cre4* mice will provide fresh insight into the role and the regulatory mechanism for HGF/Met-mediated oncogenic signaling in promoting prostate tumor development and progression.

Experimental procedures

Mouse breeding and genotyping

The founder mice were bred with WT C57Bl6/J, and progenies were genotyped to confirm the presence of the transgene. To generate conditional *Met* transgenic mice, the *LSL-Met* transgenic mice ($H11^{Met/+}$) were intercrossed with the *PB-Cre4* strain (15), carrying the *Cre* transgene under the control of a modified probasin promoter (ARR2PB) (36, 67). Mice homozygous for floxed β-catenin exon 3, $Ctnnb1^{Ex3(L)/Ex3(L)}$, were obtained from the Jackson Laboratory (Bar Harbor, ME) (strain 004597). All animals used in this study were on a C57BL/6 background, and all experiments were performed in accordance with animal care guidelines approved by the Institutional Animal Care and Use Committee at Beckman Research Institute and City of Hope.

For genotyping, mouse tail tips were incubated in lysis buffer (catalog no. 102-T, VIAGEN Biotech, Los Angeles, CA) for genomic DNA. The conditional expression of $H11^{Met/+}$ was detected with the forward 5′-AGCGCATCGCCTTCTATCG-CCTTC-3′ and reverse primers 5′-AAACAATCTGGGTGT-TCC-3′. PCR was performed as follows: 5 min at 94 °C and then 34 cycles of 94 °C for 30 s, 62 °C for 30 s, and 72 °C for 70 s, followed by a final step at 72 °C for 5 min. For *Ctnnb1(ex3)* allele, the forward (5′-AACTGGCTTTTGGTGTCGGG-3′) and reverse (5′-TCGGTGGCTTGCTGATTATTTC-3′) primers were used to distinguish the WT and floxed alleles (68). For *PB-Cre4*, the forward (5′-GCAGGAAGCTACTCTGCACC-TTG-3′) and reverse (5′-GATCCTGGCAATTTCGGCTAT-3′) primers were used (69).

In vivo prostate regeneration assay

Prostatic tissues were collected from 3-week-old mice and implanted under the renal capsule of SCID mice or *hHGFtg*

SCID mice (35, 70). The SCID or hHGFtg SCID mice were sacrificed after 12 or 8 weeks, respectively, and the grafted tissues were collected and used for histological analyses.

Western blotting

Prostates from $H11^{Met/+}$/$Ctnnb1^{(Ex3)L/+}$*PB-Cre4* and $Ctnnb1^{(Ex3)L/+}$*PB-Cre4* mice were cut into small pieces, homogenized, and isolated with radioimmune precipitation assay buffer (0.5% Nonidet P-40, 0.3% Triton X-100, 15 mM $MgCl_2$, 5 mM EDTA, 150 mM NaCl, 50 mM Tris-HCl, pH 7.8) as described previously (69, 71). Whole-cell lysates were denatured by boiling in SDS-sample buffer and then resolved by 8% SDS-PAGE. The proteins were transferred onto a nitrocellulose membrane and probed with anti-FLAG antibody (F3165, Sigma-Aldrich), anti-β-catenin (BD 610154, BD Transduction Laboratories, Sparks, MD), or anti-tubulin antibody (MS-581, Thermo Scientific). Detection was performed with ECL reagents (Amersham Biosciences).

Histological analyses and immunostaining

Mouse tissues were fixed and processed as described in our previous study (72). For histological analysis, 5-μm serial sections were processed from Clearify to water through a decreasing ethanol gradient, stained with 5% (w/v) Harris hematoxylin and eosin, and processed back to Clearify through an increasing ethanol gradient.

For immunohistochemical assays, 5-μm sections were boiled in 0.01 M citrate buffer (pH 6.0) for 20 min after rehydration from Clearify to water, placed in 0.3% H_2O_2/methanol for 15 min, and blocked by 5% goat serum or 5% donkey serum. Tissue slides were then exposed to first antibodies in PBS with 1% goat (or donkey serum) at 4 °C overnight. The following dilutions were used: 1:150 dilution of anti-MET (AF527, R&D Systems, Minneapolis, MN), 1:100 anti-pMET (3077, Cell Signaling, Danvers, MA), 1:1000 anti-mouse/human AR (PA5-16750, Invitrogen, Carlsbad, CA), 1:200 anti-E-cadherin (c20820, BD Transduction Laboratories), 1:2000 anti-CK8 (MMS-162P, Covance, Brea, CA), 1:2600 anti-CK5 (PRB-160P, Covance), 1:400 anti-Ki67 (D3B5, Cell Signaling, Danvers, MA), 1:150 anti-HGF (52445, Cell Signaling), 1:200 anti-Lef1 (sc374522, Santa Cruz Biotechnology, Dallas, TX). Tissues were then incubated with biotinylated goat anti-mouse, goat anti-rabbit (Vector Laboratories, BA-1000 or BA-9200), or donkey anti-goat (ab6987, Abcam, Cambridge, MA) at 1:750 dilution for 1 h at room temperature followed by a 45-min incubation with horseradish peroxidase–conjugated streptavidin (Vector Laboratories, SA-5004). Immunostainings were visualized using a DAB kit (Vector Laboratories, SK-4100). Slides were counterstained with hematoxylin, and coverslips were mounted with Permount Mounting Medium (SP15-500, Fisher).

RNA isolation, RNA-Seq, and RT-qPCR

RNA samples were isolated from age-matched mice of different genotypes. The prostate tissues were homogenized in RNA-Bee (TEL-TEST, Inc., Friendswood, TX), and total RNA was isolated as recommended by the manufacturer. The purified RNA libraries were then sequenced using the Illumina HiSeq 2000 at the City of Hope Integrative Genomics Core. Pathway analysis of hallmark gene sets was performed using preranked gene set enrichment analysis (GSEA 4.0.1).

RT was carried out as described in our previous report (73). For quantitative PCR, cDNA samples were mixed with Power SYBR Green qPCR Mix (4367569, Applied Biosystems) and specific primers, and quantitative PCR was performed according to the manufacturer's protocol. Relative mRNA levels were calculated by the $\Delta\Delta C(T)$ method (74). Reactions were done in triplicate, and the values were normalized by PPIA (peptidylprolyl isomerase A) expression levels. Primers for *Ccnd1* (5′-GTGACACTTATGAGCGCCCTA-3′; 5′-CCACTTGTCGCCAATCTTGTA-3′), *Lef1* (5′-CCAGCAGATTTCAAGGTGGAC-3′; 5′-TTACAGCTACCTGCCACTTTTC-3′), *Myc* (5′-CCACGCAGTGAGCATCGAA-3′; 5′-CAGGTGGCAGGTCATTTTCTT-3′), *Sox2* (5′-AGACGGACACACATGGAGGT-3′; 5′-AAAGACTCAATGCATGCCAC-3′), *Onecut2* (5′-AGACGGACACACATGGAGGT-3′; 5′-AAAGACTCAATGCATGCCAC-3′), *Sp6* (5′-AGACGGACACACATGGAGGT-3′; 5′-AAAGACTCAATGCATGCCAC-3′), and *Ppia* (5′-TGTGCCAGGGTGGTGACTTT-3′; 5′-CGTTTGTGTTTGGTCCAGCAT-3′) were synthesized and used in the qPCRs, respectively.

ChIP assays

ChIP assays were performed as described previously (75). Briefly, mouse tissues were minced and incubated with 1% formaldehyde for 15 min and quenched with 0.150 M glycine for 10 min. Samples were washed sequentially with cold PBS and resuspended in cell lysis buffer (50 mM Tris-HCl (pH 8.0), 140 mM NaCl, 1 mM EDTA, 10% glycerol, 0.5% Nonidet P-40, and 0.25% Triton X-100) and then homogenized. The chromatin was sheared in nuclear lysis buffer (10 mM Tris-HCl, pH 8.0, 1 mM EDTA, 0.5 mM EGTA, and 0.2% SDS) to an average size of 200–500 bp by sonication and then diluted 3-fold in ChIP dilution buffer (0.01% SDS, 1.1% Triton X-100, 1.2 mM EDTA, 16.7 mM Tris-HCl, pH 8.1, and 167 mM NaCl) and was subjected to immunoprecipitation by magnetic protein G beads (Invitrogen) conjugated with β-catenin (BD 610154) or Met antibody (3D4, R&D Systems, Minneapolis, MN). Cross-links were reversed, and chromatin DNA fragments were analyzed by real-time qPCR with the indicated primers: *Myc-A* (5′-ACTCATTCGTTCGTCCTTC-3′; 5′-CCTCGCTCCACACAATAC-3′); *Myc-B* (5′-CTCACTGGAACTTACAATCTG-3′; 5′-CAACGCCCAAAGGAAATC-3′); *Ccnd1* (5′-CCGGCTTTGATCTCTGCTTA-3′; 5′-CGCGGAGTCTGTAGCTCTCT-3′); *Lef1* (5′-CTGCGGGCTGGAACATTT-3′; 5′-CGGAGGAGGAGGGGAGAA-3′).

ELISA

Mouse sera were collected from different genotype mice and separated by centrifugation from total blood following cardiac puncture as described previously (38). The serum concentration of HGF was measured by the Quantikine ELISA human HGF immunoassay (DHG00B, R&D Systems). Measurements were performed in in accordance with the manufacturer's instructions.

Statistical analyses

Data are shown as the mean ± S.D. Differences between groups were examined by two-tailed Student's *t* test or two-way analysis of variance for comparisons among multiple groups. For all analyses, $p < 0.05$ was considered statistically significant.

Author contributions—J. A., J. M., A. P., W. K. K., A. O., E. H., Y. H., E.-J. Y., V. L., J. G., and Z. S. validation; J. A., J. M., W. K. K., and Z. S. investigation; J. A., J. M., A. P., W. K. K., A. O., Y. H., E.-J. Y., V. L., D.-H. L., J. G., and Z. S. methodology; J. A. and Z. S. writing-original draft; J. A., A. O., and Z. S. writing-review and editing; J. M. and Z. S. conceptualization; J. M., E. H., Y. H., V. L., D.-H. L., and Z. S. resources; J. M. and Z. S. data curation; J. M., W. K. K., A. O., E. H., E.-J. Y., V. L., and Z. S. formal analysis; J. M. and Z. S. supervision; J. M., A. P., W. K. K., A. O., Y. H., V. L., D.-H. L., J. G., and Z. S. visualization; Z. S. funding acquisition; Z. S. project administration.

References

1. DeSantis, C. E., Miller, K. D., Goding Sauer, A., Jemal, A., and Siegel, R. L. (2019) Cancer statistics for African Americans, 2019. *CA Cancer J. Clin.* **69,** 211–233 CrossRef Medline
2. Jemal, A., Bray, F., Center, M. M., Ferlay, J., Ward, E., and Forman, D. (2011) Global cancer statistics. *CA Cancer J. Clin.* **61,** 69–90 CrossRef Medline
3. Matsumoto, K., and Nakamura, T. (1996) Emerging multipotent aspects of hepatocyte growth factor. *J. Biochem.* **119,** 591–600 CrossRef Medline
4. Humphrey, P. A., Zhu, X., Zarnegar, R., Swanson, P. E., Ratliff, T. L., Vollmer, R. T., and Day, M. L. (1995) Hepatocyte growth factor and its receptor (c-MET) in prostatic carcinoma. *Am. J. Pathol.* **147,** 386–396 Medline
5. Kasai, S., Sugimura, K., Matsumoto, K., Nishi, N., Kishimoto, T., and Nakamura, T. (1996) Hepatocyte growth factor is a paracrine regulator of rat prostate epithelial growth. *Biochem. Biophys. Res. Commun.* **228,** 646–652 CrossRef Medline
6. Pisters, L. L., Troncoso, P., Zhau, H. E., Li, W., von Eschenbach, A. C., and Chung, L. W. (1995) c-met proto-oncogene expression in benign and malignant human prostate tissues. *J. Urol.* **154,** 293–298 CrossRef Medline
7. Birchmeier, C., Birchmeier, W., Gherardi, E., and Vande Woude, G. F. (2003) Met, metastasis, motility and more. *Nat. Rev. Mol. Cell Biol.* **4,** 915–925 CrossRef Medline
8. Knudsen, B. S., Gmyrek, G. A., Inra, J., Scherr, D. S., Vaughan, E. D., Nanus, D. M., Kattan, M. W., Gerald, W. L., and Vande Woude, G. F. (2002) High expression of the Met receptor in prostate cancer metastasis to bone. *Urology* **60,** 1113–1117 CrossRef Medline
9. Watanabe, M., Fukutome, K., Kato, H., Murata, M., Kawamura, J., Shiraishi, T., and Yatani, R. (1999) Progression-linked overexpression of c-Met in prostatic intraepithelial neoplasia and latent as well as clinical prostate cancers. *Cancer Lett.* **141,** 173–178 CrossRef Medline
10. van Leenders, G. J., Sookhlall, R., Teubel, W. J., de Ridder, C. M., Reneman, S., Sacchetti, A., Vissers, K. J., van Weerden, W., and Jenster, G. (2011) Activation of c-MET induces a stem-like phenotype in human prostate cancer. *PLoS One* **6,** e26753 CrossRef Medline
11. Russo, A. L., Jedlicka, K., Wernick, M., McNally, D., Kirk, M., Sproull, M., Smith, S., Shankavaram, U., Kaushal, A., Figg, W. D., Dahut, W., Citrin, D., Bottaro, D. P., Albert, P. S., Tofilon, P. J., and Camphausen, K. (2009) Urine analysis and protein networking identify met as a marker of metastatic prostate cancer. *Clin. Cancer Res.* **15,** 4292–4298 CrossRef Medline
12. Xie, Y., Lu, W., Liu, S., Yang, Q., Carver, B. S., Li, E., Wang, Y., Fazli, L., Gleave, M., and Chen, Z. (2014) Crosstalk between nuclear MET and SOX9/β-catenin correlates with castration-resistant prostate cancer. *Mol. Endocrinol.* **28,** 1629–1639 CrossRef Medline
13. Gupta, S., Li, J., Kemeny, G., Bitting, R. L., Beaver, J., Somarelli, J. A., Ware, K. E., Gregory, S., and Armstrong, A. J. (2017) Whole genomic copy number alterations in circulating tumor cells from men with abiraterone or enzalutamide-resistant metastatic castration-resistant prostate cancer. *Clin. Cancer Res.* **23,** 1346–1357 CrossRef Medline
14. Cannistraci, A., Federici, G., Addario, A., Di Pace, A. L., Grassi, L., Muto, G., Collura, D., Signore, M., De Salvo, L., Sentinelli, S., Simone, G., Costantini, M., Nanni, S., Farsetti, A., Coppola, V., *et al.* (2017) C-Met/miR-130b axis as novel mechanism and biomarker for castration resistance state acquisition. *Oncogene* **36,** 3718–3728 CrossRef Medline
15. Mi, J., Hooker, E., Balog, S., Zeng, H., Johnson, D. T., He, Y., Yu, E. J., Wu, H., Le, V., Lee, D. H., Aldahl, J., Gonzalgo, M. L., and Sun, Z. (2018) Activation of hepatocyte growth factor/MET signaling initiates oncogenic transformation and enhances tumor aggressiveness in the murine prostate. *J. Biol. Chem.* **293,** 20123–20136 CrossRef Medline
16. Tasic, B., Hippenmeyer, S., Wang, C., Gamboa, M., Zong, H., Chen-Tsai, Y., and Luo, L. (2011) Site-specific integrase-mediated transgenesis in mice via pronuclear injection. *Proc. Natl. Acad. Sci. U.S.A.* **108,** 7902–7907 CrossRef Medline
17. Wu, X., Noda, A., Noda, H., Eto, S., Muro, H., Ono, Y., and Inokuchi, K. (2001) Enantioselective metabolism of propanolol in isolated hepatocytes prepared from untreated, PB- or 3-MC-pretreated rats. *J. UOEH* **23,** 23–34 CrossRef Medline
18. Verras, M., and Sun, Z. (2006) Roles and regulation of Wnt signaling and β-catenin in prostate cancer. *Cancer Lett.* **237,** 22–32 CrossRef Medline
19. Murillo-Garzón, V., and Kypta, R. (2017) WNT signalling in prostate cancer. *Nat. Rev. Urol.* **14,** 683–696 CrossRef Medline
20. Robinson, D., Van Allen, E. M., Wu, Y.-M., Schultz, N., Lonigro, R. J., Mosquera, J.-M., Montgomery, B., Taplin, M.-E., Pritchard, C. C., Attard, G., Beltran, H., Abida, W., Bradley, R. K., Vinson, J., Cao, X., *et al.* (2015) Integrative clinical genomics of advanced prostate cancer. *Cell* **161,** 1215–1228 CrossRef Medline
21. Sun, Y., Campisi, J., Higano, C., Beer, T. M., Porter, P., Coleman, I., True, L., and Nelson, P. S. (2012) Treatment-induced damage to the tumor microenvironment promotes prostate cancer therapy resistance through WNT16B. *Nat. Med.* **18,** 1359–1368 CrossRef Medline
22. Wissmann, C., Wild, P. J., Kaiser, S., Roepcke, S., Stoehr, R., Woenckhaus, M., Kristiansen, G., Hsieh, J. C., Hofstaedter, F., Hartmann, A., Knuechel, R., Rosenthal, A., and Pilarsky, C. (2003) WIF1, a component of the Wnt pathway, is down-regulated in prostate, breast, lung, and bladder cancer. *J. Pathol.* **201,** 204–212 CrossRef Medline
23. Placencio, V. R., Sharif-Afshar, A. R., Li, X., Huang, H., Uwamariya, C., Neilson, E. G., Shen, M. M., Matusik, R. J., Hayward, S. W., and Bhowmick, N. A. (2008) Stromal transforming growth factor-β signaling mediates prostatic response to androgen ablation by paracrine Wnt activity. *Cancer Res.* **68,** 4709–4718 CrossRef Medline
24. Chesire, D. R., and Isaacs, W. B. (2002) Ligand-dependent inhibition of β-catenin/TCF signaling by androgen receptor. *Oncogene* **21,** 8453–8469 CrossRef Medline
25. Bierie, B., Nozawa, M., Renou, J. P., Shillingford, J. M., Morgan, F., Oka, T., Taketo, M. M., Cardiff, R. D., Miyoshi, K., Wagner, K. U., Robinson, G. W., and Hennighausen, L. (2003) Activation of β-catenin in prostate epithelium induces hyperplasias and squamous transdifferentiation. *Oncogene* **22,** 3875–3887 CrossRef Medline
26. Gounari, F., Signoretti, S., Bronson, R., Klein, L., Sellers, W. R., Kum, J., Siermann, A., Taketo, M. M., von Boehmer, H., and Khazaie, K. (2002) Stabilization of β-catenin induces lesions reminiscent of prostatic intraepithelial neoplasia, but terminal squamous transdifferentiation of other secretory epithelia. *Oncogene* **21,** 4099–4107 CrossRef Medline
27. Mulholland, D. J., Cheng, H., Reid, K., Rennie, P. S., and Nelson, C. C. (2002) The androgen receptor can promote β-catenin nuclear translocation independently of adenomatous polyposis coli. *J. Biol. Chem.* **277,** 17933–17943 CrossRef Medline
28. Truica, C. I., Byers, S., and Gelmann, E. P. (2000) β-Catenin affects androgen receptor transcriptional activity and ligand specificity. *Cancer Res.* **60,** 4709–4713 Medline

29. Yang, F., Li, X., Sharma, M., Sasaki, C. Y., Longo, D. L., Lim, B., and Sun, Z. (2002) Linking β-catenin to androgen-signaling pathway. *J. Biol. Chem.* **277,** 11336–11344 CrossRef Medline
30. Gundem, G., Van Loo, P., Kremeyer, B., Alexandrov, L. B., Tubio, J. M., Papaemmanuil, E., Brewer, D. S., Kallio, H. M., Högnäs, G., and Annala, M., Kivinummi, K., Goody, V., Latimer, C., O'Meara, S., Dawson, K. J., *et al.* (2015) The evolutionary history of lethal metastatic prostate cancer. *Nature* **520,** 353–357 CrossRef Medline
31. Harada, N., Tamai, Y., Ishikawa, T., Sauer, B., Takaku, K., Oshima, M., and Taketo, M. M. (1999) Intestinal polyposis in mice with a dominant stable mutation of the β-catenin gene. *EMBO J.* **18,** 5931–5942 CrossRef Medline
32. Armenia, J., Wankowicz, S. A. M., Liu, D., Gao, J., Kundra, R., Reznik, E., Chatila, W. K., Chakravarty, D., Han, G. C., Coleman, I., Montgomery, B., Pritchard, C., Morrissey, C., Barbieri, C. E., Beltran, H., *et al.* (2018) The long tail of oncogenic drivers in prostate cancer. *Nat. Genet.* **50,** 645–651 CrossRef Medline
33. Cerami, E., Gao, J., Dogrusoz, U., Gross, B. E., Sumer, S. O., Aksoy, B. A., Jacobsen, A., Byrne, C. J., Heuer, M. L., Larsson, E., Antipin, Y., Reva, B., Goldberg, A. P., Sander, C., and Schultz, N. (2012) The cBio cancer genomics portal: an open platform for exploring multidimensional cancer genomics data. *Cancer Discov.* **2,** 401–404 CrossRef Medline
34. Gao, J., Aksoy, B. A., Dogrusoz, U., Dresdner, G., Gross, B., Sumer, S. O., Sun, Y., Jacobsen, A., Sinha, R., Larsson, E., Cerami, E., Sander, C., and Schultz, N. (2013) Integrative analysis of complex cancer genomics and clinical profiles using the cBioPortal. *Sci. Signal.* **6,** pl1 CrossRef Medline
35. Lee, S. H., Luong, R., Johnson, D. T., Cunha, G. R., Rivina, L., Gonzalgo, M. L., and Sun, Z. (2016) Androgen signaling is a confounding factor for β-catenin-mediated prostate tumorigenesis. *Oncogene* **35,** 702–714 CrossRef Medline
36. Wu, X., Wu, J., Huang, J., Powell, W. C., Zhang, J., Matusik, R. J., Sangiorgi, F. O., Maxson, R. E., Sucov, H. M., and Roy-Burman, P. (2001) Generation of a prostate epithelial cell-specific Cre transgenic mouse model for tissue-specific gene ablation. *Mech. Dev.* **101,** 61–69 CrossRef Medline
37. Ittmann, M., Huang, J., Radaelli, E., Martin, P., Signoretti, S., Sullivan, R., Simons, B. W., Ward, J. M., Robinson, B. D., Chu, G. C., Loda, M., Thomas, G., Borowsky, A., and Cardiff, R. D. (2013) Animal models of human prostate cancer: the consensus report of the New York meeting of the Mouse Models of Human Cancers Consortium Prostate Pathology Committee. *Cancer Res.* **73,** 2718–2736 CrossRef Medline
38. Parasuraman, S., Raveendran, R., and Kesavan, R. (2010) Blood sample collection in small laboratory animals. *J. Pharmacol. Pharmacother.* **1,** 87–93 CrossRef Medline
39. Barrett, R. T., Erikstad, K. E., Sandvik, H., Myksvoll, M., Jenni-Eiermann, S., Kristensen, D. L., Moum, T., Reiertsen, T. K., and Vikebø, F. (2015) The stress hormone corticosterone in a marine top predator reflects short-term changes in food availability. *Ecol. Evol.* **5,** 1306–1317 CrossRef Medline
40. Bhardwaj, A., Rao, M. K., Kaur, R., Buttigieg, M. R., and Wilkinson, M. F. (2008) GATA factors and androgen receptor collaborate to transcriptionally activate the Rhox5 homeobox gene in Sertoli cells. *Mol. Cell Biol.* **28,** 2138–2153 CrossRef Medline
41. Chang, W. C., Chou, C. K., Tsou, C. C., Li, S. H., Chen, C. H., Zhuo, Y. X., Hsu, W. L., and Chen, C. H. (2010) Comparative proteomic analysis of proteins involved in the tumorigenic process of seminal vesicle carcinoma in transgenic mice. *Int. J. Proteomics* **2010,** 726968 CrossRef Medline
42. Chen, C., Zhang, Q., Liu, S., Parajuli, K. R., Qu, Y., Mei, J., Chen, Z., Zhang, H., Khismatullin, D. B., and You, Z. (2015) IL-17 and insulin/IGF1 enhance adhesion of prostate cancer cells to vascular endothelial cells through CD44-VCAM-1 interaction. *Prostate* **75,** 883–895 CrossRef Medline
43. Chen, K., Luo, Z., Li, Z., Liu, Y., and Zhao, Q. (2011) PERP gene therapy attenuates lung cancer xenograft via inducing apoptosis and suppressing VEGF. *Cancer Biol. Ther.* **12,** 1114–1119 CrossRef Medline
44. Chimento, A., Sirianni, R., Casaburi, I., Ruggiero, C., Maggiolini, M., Andò, S., and Pezzi, V. (2012) 17β-Estradiol activates GPER- and ESR1-dependent pathways inducing apoptosis in GC-2 cells, a mouse spermatocyte-derived cell line. *Mol. Cell Endocrinol.* **355,** 49–59 CrossRef Medline
45. De Marzo, A. M., Platz, E. A., Sutcliffe, S., Xu, J., Grönberg, H., Drake, C. G., Nakai, Y., Isaacs, W. B., and Nelson, W. G. (2007) Inflammation in prostate carcinogenesis. *Nat. Rev. Cancer* **7,** 256–269 CrossRef Medline
46. Ding, Z., Wu, C. J., Chu, G. C., Xiao, Y., Ho, D., Zhang, J., Perry, S. R., Labrot, E. S., Wu, X., Lis, R., Hoshida, Y., Hiller, D., Hu, B., Jiang, S., Zheng, H., *et al.* (2011) SMAD4-dependent barrier constrains prostate cancer growth and metastatic progression. *Nature* **470,** 269–273 CrossRef Medline
47. Hahn-Strömberg, V., Askari, S., Befekadu, R., Matthiessen, P., Karlsson, S., and Nilsson, T. K. (2014) Polymorphisms in the CLDN1 and CLDN7 genes are related to differentiation and tumor stage in colon carcinoma. *APMIS* **122,** 636–642 CrossRef Medline
48. Katoh, M., and Katoh, M. (2003) CLDN23 gene, frequently down-regulated in intestinal-type gastric cancer, is a novel member of CLAUDIN gene family. *Int. J. Mol. Med.* **11,** 683–689 Medline
49. Kim, J. H., Kim, T. W., and Kim, S. J. (2011) Downregulation of ARFGEF1 and CAMK2B by promoter hypermethylation in breast cancer cells. *BMB Rep.* **44,** 523–528 CrossRef Medline
50. Kozakowski, N., Hartmann, C., Klingler, H. C., Susani, M., Mazal, P. R., Scharrer, A., and Haitel, A. (2014) Immunohistochemical expression of PDGFR, VEGF-C, and proteins of the mToR pathway before and after androgen deprivation therapy in prostate carcinoma: significant decrease after treatment. *Target Oncol.* **9,** 359–366 CrossRef Medline
51. Kurashige, J., Sawada, G., Takahashi, Y., Eguchi, H., Sudo, T., Ikegami, T., Yoshizumi, T., Soejima, Y., Ikeda, T., Kawanaka, H., Uchiyama, H., Yamashita, Y., Morita, M., Oki, E., Saeki, H., Sugimachi, K., Watanabe, M., Mori, M., Baba, H., and Mimori, K. (2013) Suppression of MAL gene expression in gastric cancer correlates with metastasis and mortality. *Fukuoka Igaku Zasshi* **104,** 344–349 Medline
52. Lee, J., Beliakoff, J., and Sun, Z. (2007) The novel PIAS-like protein hZimp10 is a transcriptional co-activator of the p53 tumor suppressor. *Nucleic Acids Res.* **35,** 4523–4534 CrossRef Medline
53. Mulholland, D. J., Kobayashi, N., Ruscetti, M., Zhi, A., Tran, L. M., Huang, J., Gleave, M., and Wu, H. (2012) Pten loss and RAS/MAPK activation cooperate to promote EMT and metastasis initiated from prostate cancer stem/progenitor cells. *Cancer Res.* **72,** 1878–1889 CrossRef Medline
54. Rao, D. S., Hyun, T. S., Kumar, P. D., Mizukami, I. F., Rubin, M. A., Lucas, P. C., Sanda, M. G., and Ross, T. S. (2002) Huntingtin-interacting protein 1 is overexpressed in prostate and colon cancer and is critical for cellular survival. *J. Clin. Invest.* **110,** 351–360 CrossRef Medline
55. Saeki, N., Usui, T., Aoyagi, K., Kim, D. H., Sato, M., Mabuchi, T., Yanagihara, K., Ogawa, K., Sakamoto, H., Yoshida, T., and Sasaki, H. (2009) Distinctive expression and function of four GSDM family genes (GSDMA-D) in normal and malignant upper gastrointestinal epithelium. *Genes Chromosomes Cancer* **48,** 261–271 CrossRef Medline
56. Sasnauskienė, A., Jonušienė, V., Krikštaponienė, A., Butkytė, S., Dabkevičienė, D., Kanopienė, D., Kazbarienė, B., and Didžiapetrienė, J. (2014) NOTCH1, NOTCH3, NOTCH4, and JAG2 protein levels in human endometrial cancer. *Medicina* **50,** 14–18 CrossRef Medline
57. Sathyanarayana, U. G., Padar, A., Suzuki, M., Maruyama, R., Shigematsu, H., Hsieh, J. T., Frenkel, E. P., and Gazdar, A. F. (2003) Aberrant promoter methylation of laminin-5-encoding genes in prostate cancers and its relationship to clinicopathological features. *Clin. Cancer Res.* **9,** 6395–6400 Medline
58. Singh, V., Singh, L. C., Vasudevan, M., Chattopadhyay, I., Borthakar, B. B., Rai, A. K., Phukan, R. K., Sharma, J., Mahanta, J., Kataki, A. C., Kapur, S., and Saxena, S. (2015) Esophageal cancer epigenomics and integrome analysis of genome-wide methylation and expression in high risk Northeast Indian population. *OMICS* **19,** 688–699 CrossRef Medline
59. Stucke, V. M., Timmerman, E., Vandekerckhove, J., Gevaert, K., and Hall, A. (2007) The MAGUK protein MPP7 binds to the polarity protein hDlg1 and facilitates epithelial tight junction formation. *Mol. Biol. Cell* **18,** 1744–1755 CrossRef Medline
60. Vadnais, C., Shooshtarizadeh, P., Rajadurai, C. V., Lesurf, R., Hulea, L., Davoudi, S., Cadieux, C., Hallett, M., Park, M., and Nepveu, A. (2014) Autocrine cctivation of the Wnt/β-catenin pathway by CUX1 and GLIS1 in breast cancers. *Biol. Open* **3,** 937–946 CrossRef Medline

61. Mahmoudi, T., Boj, S. F., Hatzis, P., Li, V. S., Taouatas, N., Vries, R. G., Teunissen, H., Begthel, H., Korving, J., Mohammed, S., Heck, A. J., and Clevers, H. (2010) The leukemia-associated Mllt10/Af10-Dot1l are Tcf4/β-catenin coactivators essential for intestinal homeostasis. *PLoS Biol.* **8,** e1000539 CrossRef Medline
62. Wyce, A., Bai, Y., Nagpal, S., and Thompson, C. C. (2010) Research resource: the androgen receptor modulates expression of genes with critical roles in muscle development and function. *Mol. Endocrinol.* **24,** 1665–1674 CrossRef Medline
63. Zhang, Y. W., Su, Y., Lanning, N., Gustafson, M., Shinomiya, N., Zhao, P., Cao, B., Tsarfaty, G., Wang, L. M., Hay, R., and Vande Woude, G. F. (2005) Enhanced growth of human met-expressing xenografts in a new strain of immunocompromised mice transgenic for human hepatocyte growth factor/scatter factor. *Oncogene* **24,** 101–106 CrossRef Medline
64. Varkaris, A., Corn, P. G., Gaur, S., Dayyani, F., Logothetis, C. J., and Gallick, G. E. (2011) The role of HGF/c-Met signaling in prostate cancer progression and c-Met inhibitors in clinical trials. *Expert Opin. Investig. Drugs* **20,** 1677–1684 CrossRef Medline
65. Jeffers, M. F., and Vande Woude, G. F. (1999) Activating mutations in the Met receptor overcome the requirement for autophosphorylation of tyrosines crucial for wild type signaling. *Oncogene* **18,** 5120–5125 CrossRef Medline
66. Rotinen, M., You, S., Yang, J., Coetzee, S. G., Reis-Sobreiro, M., Huang, W. C., Huang, F., Pan, X., Yáñez, A., Hazelett, D. J., Chu, C. Y., Steadman, K., Morrissey, C. M., Nelson, P. S., Corey, E., *et al.* (2018) ONECUT2 is a targetable master regulator of lethal prostate cancer that suppresses the androgen axis. *Nat. Med.* **24,** 1887–1898 CrossRef Medline
67. Chlenski, A., Nakashiro, K., Ketels, K. V., Korovaitseva, G. I., and Oyasu, R. (2001) Androgen receptor expression in androgen-independent prostate cancer cell lines. *Prostate* **47,** 66–75 CrossRef Medline
68. Kwak, M. K., Johnson, D. T., Zhu, C., Lee, S. H., Ye, D. W., Luong, R., and Sun, Z. (2013) Conditional deletion of the Pten gene in the mouse prostate induces prostatic intraepithelial neoplasms at early ages but a slow progression to prostate tumors. *PLoS One* **8,** e53476 CrossRef Medline
69. Yu, E. J., Hooker, E., Johnson, D. T., Kwak, M. K., Zou, K., Luong, R., He, Y., and Sun, Z. (2017) LZTS2 and PTEN collaboratively regulate ss-catenin in prostatic tumorigenesis. *PLoS One* **12,** e0174357 CrossRef Medline
70. Lee, S. H., Johnson, D. T., Luong, R., Yu, E. J., Cunha, G. R., Nusse, R., and Sun, Z. (2015) Wnt/β-catenin-responsive cells in prostatic development and regeneration. *Stem Cells* **33,** 3356–3367 CrossRef Medline
71. Sharma, M., Chuang, W. W., and Sun, Z. (2002) Phosphatidylinositol 3-kinase/Akt stimulates androgen pathway through GSK3β inhibition and nuclear β-catenin accumulation. *J. Biol. Chem.* **277,** 30935–30941 CrossRef Medline
72. Zhu, C., Luong, R., Zhuo, M., Johnson, D. T., McKenney, J. K., Cunha, G. R., and Sun, Z. (2011) Conditional expression of the androgen receptor induces oncogenic transformation of the mouse prostate. *J. Biol. Chem.* **286,** 33478–33488 CrossRef Medline
73. Hohaus, S., Petrovick, M. S., Voso, M. T., Sun, Z., Zhang, D. E., and Tenen, D. G. (1995) PU.1 (Spi-1) and C/EBPα regulate expression of the granulocyte- macrophage colony-stimulating factor receptor α gene. *Mol. Cell Biol.* **15,** 5830–5845 CrossRef Medline
74. Livak, K. J., and Schmittgen, T. D. (2001) Analysis of relative gene expression data using real-time quantitative PCR and the $2(-\Delta\Delta C(T))$ method. *Methods* **25,** 402–408 CrossRef Medline
75. Cotney, J. L., and Noonan, J. P. (2015) Chromatin immunoprecipitation with fixed animal tissues and preparation for high throughput sequencing. *Cold Spring Harb Protoc* **2,** 191–199 CrossRef Medline